

Alternative Splicing and Transcriptome Profiling of Experimental Autoimmune Encephalomyelitis Using Genome-Wide Exon Arrays

Alan Gillett^{1*}, Klio Maratou², Chris Fewings², Robert A. Harris¹, Maja Jagodic¹, Tim Aitman², Tomas Olsson¹

¹ Department of Clinical Neuroscience, Karolinska Institutet, Neuroimmunology Unit, Center for Molecular Medicine, Karolinska Hospital at Solna, Stockholm, Sweden,

² Clinical Sciences Centre, Physiological Genomics and Medicine Group, Hammersmith Hospital, London, United Kingdom

Abstract

Background: Multiple Sclerosis (MS) is a chronic inflammatory disease causing demyelination and nerve loss in the central nervous system. Experimental autoimmune encephalomyelitis (EAE) is an animal model of MS that is widely used to investigate complex pathogenic mechanisms. Transcriptional control through isoform selection and mRNA levels determines pathway activation and ultimately susceptibility to disease.

Methodology/Principal Findings: We have studied the role of alternative splicing and differential expression in lymph node cells from EAE-susceptible Dark Agouti (DA) and EAE-resistant Piebald Virol Glaxo.AV1 (PVG) inbred rat strains using Affymetrix Gene Chip Rat Exon 1.0 ST Arrays. Comparing the two strains, we identified 11 differentially spliced and 206 differentially expressed genes at day 7 post-immunization, as well as 9 differentially spliced and 144 differentially expressed genes upon autoantigen re-stimulation. Functional clustering and pathway analysis implicate genes for glycosylation, lymphocyte activation, potassium channel activity and cellular differentiation in EAE susceptibility.

Conclusions/Significance: Our results demonstrate that alternative splicing occurs during complex disease and may govern EAE susceptibility. Additionally, transcriptome analysis not only identified previously defined EAE pathways regulating the immune system, but also novel mechanisms. Furthermore, several identified genes overlap known quantitative trait loci, providing novel causative candidate targets governing EAE.

Citation: Gillett A, Maratou K, Fewings C, Harris RA, Jagodic M, et al. (2009) Alternative Splicing and Transcriptome Profiling of Experimental Autoimmune Encephalomyelitis Using Genome-Wide Exon Arrays. PLoS ONE 4(11): e7773. doi:10.1371/journal.pone.0007773

Editor: Juan Valcarcel, Centre de Regulació Genòmica, Spain

Received: August 17, 2009; **Accepted:** October 12, 2009; **Published:** November 10, 2009

Copyright: © 2009 Gillett et al. This is an open-access article distributed under the terms of the Creative Commons Attribution License, which permits unrestricted use, distribution, and reproduction in any medium, provided the original author and source are credited.

Funding: This work was supported by the 6th Framework Program of the European Union, EURATools (LSHG-CT-2005-019015) and Neuropromise (LSHM-CT-2005-018637), the Swedish Research Council, Söderberg Foundation, The Montel Williams MS Foundation and the Multiple Sclerosis Society of Canada. The funders had no role in study design, data collection and analysis, decision to publish, or preparation of the manuscript.

Competing Interests: The authors have declared that no competing interests exist.

* E-mail: Alan.Gillett@ki.se

Introduction

Multiple Sclerosis (MS) is a complex chronic inflammatory disease primarily affecting young adults. Patients experience deregulated inflammation in the periphery leading to the generation of autoreactive cells that migrate to the target organ, the central nervous system (CNS) [1]. The triggers and factors determining the underlying pathogenic peripheral immune response are unknown; however, modulation of the immune system and lymphocyte trafficking both serve to perturb disease. Use of general immunosuppressive drugs such as mitoxantrone, depleting antibodies against B-cells or antibodies that prevent CNS infiltration all reduce clinical disease [2,3,4]. Despite this, secondary damage to neurons and axons causes a progressive disability with no currently effective therapeutic options [5].

Myelin oligodendrocyte glycoprotein (MOG)-induced experimental autoimmune encephalomyelitis (EAE) is an animal model of MS with similarities in pathogenicity and histopathology [6]. Inbred rat strains differ in their susceptibility to disease, permitting

the study of susceptible genetic determinants and pathogenic mechanisms that give insight into human MS. We previously described the disease kinetics of EAE-susceptible Dark Agouti (DA) and major histocompatibility complex (MHC)-identical but EAE-resistant Piebald Virol Glaxo.AV1 (PVG) rats in peripheral lymph nodes and the spinal cord [7]. We recorded differences in T helper (T_H) cell differentiation and regulation of inflammatory markers in lymph nodes at day 7 post-EAE induction. We also characterized effector functions following re-stimulation with autoantigen. However, our previous work only focused on known disease-associated pathways including T_H1 [8] and T_H17 [9].

Many studies suggest EAE susceptibility and disease mechanisms are regulated at the level of transcription. Differential expression of genes related to antigen processing and presentation [10], chemokines, cytokines and apoptosis [11], as well as extracellular matrix, cell adhesion molecules and molecules involved in cell division, death and transcription [12], have all been reported. Several of these pathways have also been identified in MS [13,14,15]. Furthermore, alternative splicing of genes may

result in altered function important for disease pathogenesis. The MS associated interleukin-7 receptor (*IL-7R*) gene [16] is suspected to be involved in MS etiology through the differential splicing of membrane-bound and soluble forms [17]. However, genome-wide investigation of alternative splicing in MS or EAE has not yet been addressed.

In this study we carried out a well powered study of the EAE-susceptible DA and EAE-resistant PVG strains using Affymetrix GeneChip Rat Exon 1.0 ST Arrays to assess exon- and gene-level expression differences in *ex vivo* and MOG re-stimulated lymph node cells. We identify several genes that are alternatively spliced between the strains and may govern disease-driving pathways. In addition, we examine expression differences identifying novel candidates and pathways that associate with disease induction and effector phase functions. Furthermore, several of the genes overlap known quantitative trait loci (QTLs), providing novel candidate targets controlling EAE susceptibility.

Materials and Methods

Ethics Statement

All experiments in this study were approved and performed in accordance with the guidelines from the Swedish National Board for Laboratory Animals and the European Community Council Directive (86/609/EEC) under the ethical permit N332/06 entitled 'Genetic regulation, pathogenesis and therapy of EAE, an animal model for multiple sclerosis', which was approved by the North Stockholm Animal Ethics Committee (Stockholms norra djurförsöksetiska nämnd). Rats were tested according to a health-monitoring program at the National Veterinary Institute (Statens Veterinärmedicinska Anstalt, SVA) in Uppsala, Sweden.

Animals and EAE Induction

Inbred DA rats were originally obtained from the Zentralinstitut für Versuchstierzucht (Hannover, Germany) and MHC-identical PVG rats from Harlan UK Limited (Blackthorn, UK). Animals were bred in the animal facility at Karolinska Hospital (Stockholm, Sweden) in a pathogen-free and climate-controlled environment in polystyrene cages containing aspen wood shavings with free access to standard rodent chow and water with regulated 12-hour light/dark cycles. MOG, amino acids 1-125 from the N terminus, was expressed in *Escherichia coli* and purified to homogeneity by chelate chromatography [18]. The purified protein, dissolved in 6M urea, was dialyzed against phosphate buffered saline (PBS) to obtain a physiological preparation that was stored at -20°C . Female rat's aged 10–12 weeks were anaesthetized with isoflurane (Forene, Abbott Laboratories, Chicago, IL, USA) and injected subcutaneously in the tail base in order to induce EAE with a 200 μl inoculum containing 15 μg MOG in PBS, emulsified 1:1 with incomplete Freund's adjuvant (Sigma-Aldrich, St. Louis, MO, USA).

Tissue Collection and Cell Culture

Animals were sacrificed using CO_2 7 days post-EAE induction, before debut of clinical disease signs. Draining inguinal lymph nodes were collected and placed in DMEM (Gibco-BRL, Grand Island, NY, USA) enriched with 5% fetal calf serum, 1% L-glutamine, 1% penicillin-streptomycin, 1% pyruvic acid (all from Life Technologies, Paisley, Scotland) and 50 μM 2-Mercaptoethanol ('complete media'; Gibco-BRL) before being mechanically separated by passage through a mesh screen with the bolus of a syringe. Cells were spun at 300 g, resuspended in complete media and 20×10^6 cells were plated in 10 cm Nunclon Delta Surface Petri Dishes (Nunc, Roskilde, Denmark). Cultures were stimulated

for 24 hrs with 25 $\mu\text{g}/\text{ml}$ of the encephalogenic MOG_{91–108} peptide (PPR, Downton, UK). Following stimulation the cultured cells were resuspended, washed with PBS, spun and resuspended in 1 ml of TRIzol (Invitrogen, Carlsband, CA, USA). Cells that were not allocated to cell culture (greater than 12×10^6) were washed with PBS, spun and resuspended in 1 ml of TRIzol. Samples were snap frozen in liquid nitrogen and stored at -70°C .

Flow Cytometry

Lymph node cells were washed with cold PBS and resuspended in a further 100 μl of PBS. Cells were stained for 20 min at 4°C with the following antibodies: CD3-APC, CD4-PE, CD8a-PE, and CD45RA-PE:Cy5 (all from BD Biosciences, San Jose, CA, USA). Staining was visualized on a FACS Calibur (BD, Franklin Lakes, NJ, USA) with Cell Quest (version 3.2.1f1, BD) and analyzed using FlowJo (version 8.8; Tree Star Inc., Ashland, Oregon).

Exon Sequencing

Genomic DNA was isolated using a standard protocol. PCR was performed with primers surrounding differentially spliced exons. The amplified products were run on a 1% agarose (Sigma-Aldrich) electrophoresis gel. Bands were extracted and purified using a QIAquick Gel Extraction Kit (Qiagen, Valencia, CA, USA). Sequencing reactions were done at MWG (Ebersberg, Germany). Alignment was performed in Vector NTI Advance v.10 (Invitrogen).

Quantitative Real-Time PCR

Lymph node *ex vivo* or *in vitro* stimulated cells were washed with PBS before being resuspended in RLT buffer (Qiagen). RNA was purified using an RNeasy kit (Qiagen) and cDNA subsequently prepared using the iScript kit (Bio-Rad, Hercules, CA, USA). Quantitative real-time PCR (qPCR) was performed using a BioRad iQ5 iCycler Detection System with a two-step PCR protocol (95°C for 10 min followed by 40 cycles of 95°C for 10 sec and 60°C for 30 sec), using SYBR Green (Bio-Rad) as the fluorophore. Relative expression levels, corrected for amplification efficiency, were analyzed using iQ5 v2.0 software (BioRad). The primers used for SYBR Green reactions are listed in Table S1. Mann-Whitney non-parametric tests were performed using GraphPad Prism 5 (GraphPad Software, San Diego, CA, USA).

RNA Extraction and Array Hybridization

Total RNA was extracted using TRIzol reagent, and further purified and DNase I treated using an RNeasy Mini kit (Qiagen) and RNase-Free DNase Set (Qiagen), according to the manufacturer protocols. RNA concentration and purity was determined through measurement of A260/A280 ratios with a NanoDrop ND-1000 Spectrophotometer (NanoDrop Technologies, Wilmington, DE, USA). Confirmation of RNA quality was assessed using the Agilent 2100 Bioanalyzer (Agilent Technologies, Santa Clara, CA, USA). RNA samples were immediately frozen and stored at -80°C . 1 μg of total RNA was used for each sample. Target labeling, as well as array hybridization, washing and staining were performed as described in the GeneChip Whole Transcript (WT) Sense Target Labeling manual (<http://www.affymetrix.com>). Arrays were scanned using the GeneChip Scanner 3000 7G (Affymetrix).

Data Analysis

The microarray data is available in MIAME-compliant (minimum information about a microarray experiment) format at the ArrayExpress database (<http://www.ebi.ac.uk/arrayexpress>) [19]

under accession code E-MEXP-2237. CEL intensity files were produced using GeneChip Operating Software version 1.4 (Affymetrix) and quality tested using the Affymetrix Expression Console. All 16 files were deemed suitable for further study. Probe-level data were normalized using Robust Multi-array Average (RMA) [20]. Detection of alternative splicing events was performed using three parallel approaches: 1) Calculations of Microarray Detection of Alternative Splicing (MiDAS; Alternative Transcript Analysis Methods for Exon Arrays; Affymetrix-White-Paper); 2) Rank Product of Splice Index [21] (100 permutations) were performed in R v2.6.2 with the Bioconductor v2.4 [22] package OneChannelGUI v1.4.5 [23]; 3) An Alternative Splice ANOVA model implemented in Partek Genomics Suite v6.4 (Partek Incorporated, St.Louis, MO, USA) together with a filter to select for probe-sets showing significant alternative splicing score, determined at a 5% False Discovery Rate (FDR) [24], and no differential expression at gene level (transcript $p > 0.05$). Transcripts that were significant from all three approaches were visually inspected in the Partek's Gene View to generate lists of alternative splicing candidates. Detection of differential expression at the gene level was performed in Partek Genomics Suite 6.4 (Partek Incorporated). Data was summarized at the gene level using a One-Step Tukey's Biweight Algorithm, which reduces the effect of outlier probe-sets (Statistical Algorithms Description Document; Affymetrix-White-Paper). An ANOVA model, using strain, condition and batch as co-factors, was used to generate raw p values, while FDR was used for multiple test corrections. Genes with 5% FDR were classified as differentially expressed.

Functional Association Analysis

The lists of differentially expressed genes were uploaded into The Database for Annotation, Visualization and Integrated Discovery v6 (DAVID; <http://david.abcc.ncifcrf.gov/>) [25,26] to determine differentially regulated pathways using the full rat genome as reference background. Data were analyzed in the "Functional Annotation Clustering" tool using the "High" classification stringency setting for Molecular Function (MF) and Biological Process (BP) Gene Ontology (GO) terms. Functional annotation clusters with enrichment scores > 1.3 were considered significant, in accordance with DAVID recommendations [26]. Pathway analysis was also performed using non-parametric Gene Set Enrichment Analysis (GSEA), v.2 [27]. GSEA considers and ranks all genes in an experiment (not only those above an arbitrary cutoff). It then tests if the list of ranked genes is significantly enriched for pre-defined groups of genes, or "gene sets". For these analysis 1191 gene sets were used, which comprise the entire C5/GO gene sets collection of MSigDB version 2.5 [27], plus a subset of the C2/curated gene sets collection. For the latter, gene sets from the following contributors were used: Biocarta, GO, GenMAPP, KEGG, Sigma-Aldrich, Signaling transduction KE and Signaling Alliance. GSEA was run with default settings (1000 gene set permutations). Gene sets with 5% FDR were considered significant in accordance with GSEA recommendations (GSEA user guide; <http://www.broad.mit.edu/gsea/doc/GSEAUUserGuideFrame.html>).

Results

Experimental Design

DA and PVG rats were immunized with MOG to induce EAE. MHC-identical rat strains were used in order to investigate the role of non-MHC influences in alternative splicing and differential expression during EAE. After 7 days of the autoimmune response inguinal lymph nodes were extracted from 4 animals of each strain. Lymph node cells were divided into two

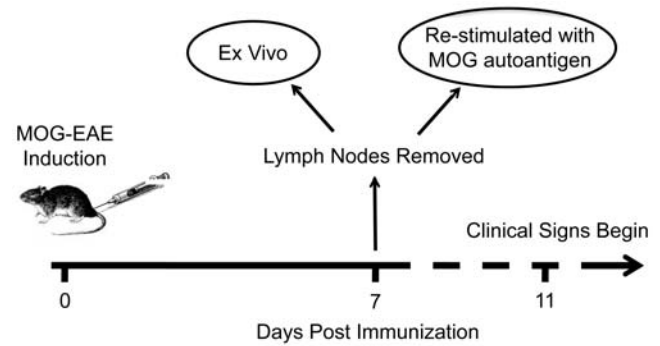


Figure 1. Experimental design. DA ($n=4$) and PVG ($n=4$) female rats were immunized with MOG (day 0) to induce EAE. At day 7, before clinical symptoms, lymph nodes were extracted and either directly harvested (*ex vivo*) or stimulated with autoantigen (MOG re-stimulated). cRNA was prepared and gene expression tested using 16 Affymetrix Rat Exon 1.0 ST Arrays. doi:10.1371/journal.pone.0007773.g001

conditions: (i) direct *ex vivo* and (ii) MOG re-stimulation (Figure 1). No differences between strains in lymphocyte types ($CD3^+$, $CD4^+$, $CD8^+$ T cells or $CD45RA^+$ B cells) were detected using flow cytometry (Figure 2). The day 7 *ex vivo* cells represent an early disease stage when the immune response towards antigen has been mounted in the draining lymph node, but before leukocyte infiltration into the CNS and clinical signs are evident. MOG re-stimulation mimics the encounter between autoreactive cells and their target in the CNS, where effector molecules such as interferon- γ (IFN- γ), interleukin-17 (IL-17) and IL-22 become up-regulated [7].

Alternative Splicing between Susceptible and Resistant Strains in EAE

We investigated the role that alternative splicing plays in EAE induction and susceptibility using three parallel analytic approaches: MiDAS, Rank Product of the Splice Index and an Alternative Splicing ANOVA, followed by visual filtering. We first compared exon expression from the DA vs. PVG day 7 *ex vivo* conditions. 11 candidate genes for alternative splicing were identified (Table 1; Figure S1). We used the Ensembl (<http://www.ensembl.org>) and Interpro (<http://www.ebi.ac.uk/interpro>) databases to evaluate if

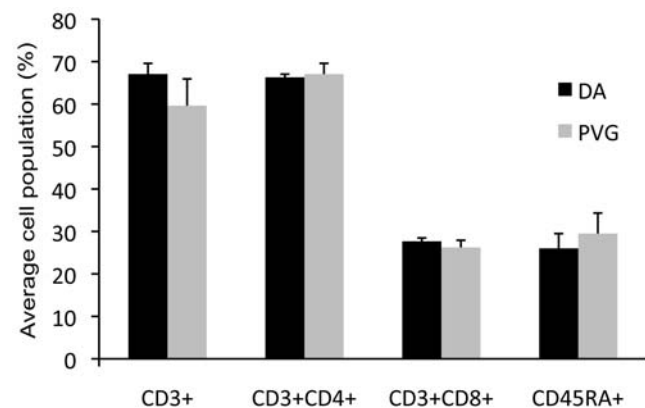


Figure 2. Cell types from lymph nodes 7 days after immunization. DA ($n=4$) and PVG ($n=4$) have equivalent proportions of $CD3^+$ T cells as well as the $CD4^+$ and $CD8^+$ subsets, in addition to equal $CD45RA^+$ B cells. Error bars represent standard deviation. doi:10.1371/journal.pone.0007773.g002

Table 1. Alternatively spliced genes between DA and PVG rats in day 7 *ex vivo* lymph nodes.

Ensembl ID	Transcript ID	Gene Symbol	p-value	Differential Exon	Reduced Strain	Interpro Domain	Domain Function
T00000032767	7271202	Itp2	7.01E-26	15	PVG	-	No specific domain
T00000017813	7354298	Nab1	4.14E-17	3	PVG	IPR006986	Nab1, negative regulation of transcription
T00000014289	7283429	Nsmaf	2.99E-13	12	DA	IPR000409	Beige/Beach, unknown
T00000005280	7112632	Tor1aip1	9.72E-12	2	DA	IPR008662	Lamina-assoc polypeptide 1C, membrane attachment
T00000009517	7248004	P-Rex1	1.64E-11	34	DA	IPR001849	Pleckstrin homology, intracellular signaling
T00000040922	7173094	Rock1	5.90E-10	12	PVG	IPR011009	Protein kinase-like, phosphotransfer
T00000036931	7198657	Dnttip2	1.99E-09	2	DA	-	Coil, coil domain
T00000026725	7282342	Cpsf3l	2.00E-09	5	PVG	IPR001279	Beta-lactamase-like, hydrolase
T00000059034	7185469	Ddx19a	1.51E-07	10	DA	-	No specific domain
T00000046251	7201908	Rasa1	3.17E-07	2 and 3	PVG	IPR001936	Ras GTPase-activating protein, signaling
T00000019338	7056128	Btbd10	2.34E-06	5	PVG	IPR003131	Potassium channel, voltage dependent

Differential Exon - alternatively spliced between strains; Reduced Strain - lower expression of indicated exon; Interpro Domain - protein domain encoded in alternatively spliced exon.
doi:10.1371/journal.pone.0007773.t001

the alternate isoforms may lack important protein functions. The isoforms for 9 of the 11 genes had putative altered protein function. The alternative splicing analysis was confirmed and quantified between strains using qPCR with primers designed for specific isoforms of each candidate (Figure 3). *Itp2* isoforms were constitutively expressed for each strain in naïve and immunized lymph node cells (Figure 3A) while all other candidates except *Ddx19a* displayed EAE-specific regulation, as naïve lymph node cells did not display the same isoform expression patterns.

We next tested if alternative splicing was involved after MOG re-stimulation, which mimics the autoantigen re-encounter that occurs when autoreactive cells migrate to the CNS. We compared DA vs. PVG MOG re-stimulated exon expression and identified 9 alternatively spliced genes; 3 of which (*Uyf1*, *Tmem41B* and *Slc24a6*) were MOG-re-stimulation specific (Table 2; Figure S2). We confirmed the Affymetrix results using qPCR for each of the candidate genes (Figure 3). The isoforms for 6 of the 9 genes had putative altered protein function. We then compared the two strains individually (i.e. *ex vivo* vs. MOG re-stimulated for DA and PVG separately). We identified a single alternatively spliced gene between DA conditions, the acetylcholine receptor ϵ subunit (*Chme*; $p = 7.77E-11$; Figure S3A). The last 2 exons at the 3' end were reduced after re-stimulation and would result in the loss of the signaling peptide. A single alternatively spliced gene was identified when comparing PVG conditions, the cAMP response element modulator (*Crem*; $p = 1.95E-06$; Figure S3B). The first 2 exons at the 5' end were reduced after re-stimulation although no specific domain is associated with this portion of the gene.

Mismatches between a microarray probe and its target sequence affect hybridization that cause erroneous probe signal estimates [28]. To determine if genetic differences (single nucleotide polymorphisms for instance) have affected our alternative splicing detection rates, we sequenced the exons of 4 genes that were alternatively spliced in both *ex vivo* and re-stimulated conditions. No genetic variation was discovered in *Itp2*, *Nsmaf* and *Cpsf3l* (data not included). However, a SNP was found in probe-set 5733439 of

Ddx19a exon 10, which could affect intensity values (Figure S4A). Accordingly, we could not reproduce the *Ddx19a* exon 10 Affymetrix data using qPCR (Figure S4B).

Differential Expression and Pathway Regulation between Susceptible and Resistant Strains

To assess EAE-relevant genes we compared day 7 *ex vivo* expression between EAE-susceptible DA and EAE-resistant PVG rats. At a 5% FDR cut-off margin 206 transcripts were differentially expressed (Table S2). DAVID clustering analysis identified five biological pathways that were significantly affected during early EAE stages: glycosylation, apoptosis, synaptic transmission, extracellular structure organization and cellular differentiation (Table 3). GSEA identified a single functional gene set, sulfotransferase activity, which was enriched in PVG *ex vivo* lymphocytes after correcting for multiple hypothesis testing (Table 4). Interestingly, two additional gene sets that fell just short of the significance threshold were also positively associated with PVG *ex vivo* lymphocytes. They contained genes involved in neuroactive ligand-receptor interaction and substrate specific channel activity.

In vitro MOG re-stimulation of autoreactive cells from peripheral lymphoid tissue replicates the pathogenic reaction occurring in the CNS of affected rats and results in the up-regulation of disease-driving effector molecules. Comparing the two strains for expression differences after MOG re-stimulation, 144 genes were significant using 5% FDR (Table S3). DAVID clustering analysis identified 8 biological pathways that were regulated between the two strains upon MOG re-stimulation, including T cell activation, apoptosis and transport (Table 5). In addition, GSEA analysis highlighted that PVG cells up-regulated of a range of potassium channel genes (Table 4).

We next examined genes that were differentially expressed upon autoantigen re-stimulation for each strain separately. Comparing DA day 7 *ex vivo* versus DA MOG re-stimulated conditions, 903 genes showed differential expression using 5% FDR (Table S4), while the same comparison for PVG identified 1356 differentially

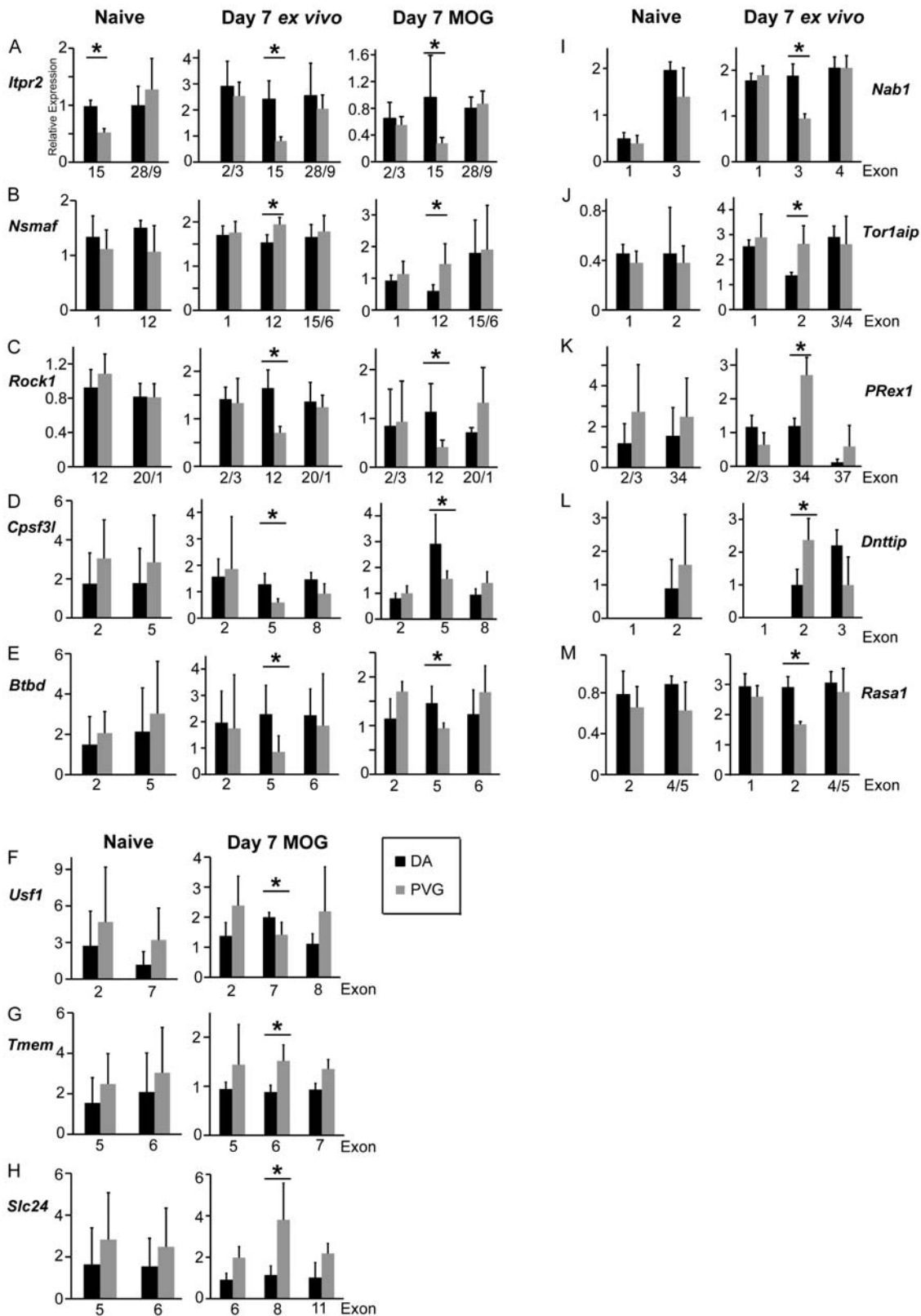


Figure 3. Quantitative PCR confirmation of alternative splicing identified constitutive and EAE-specific isoforms. Relative expression compared to *Hprt* from DA (n=4) and PVG (n=4) naïve (A–E and I–M), day 7 post-immunization (A–E and I–M) and MOG re-stimulated (A–H) conditions for selected target exons of alternatively spliced candidate genes. *Itpr2* had constitutive isoforms while all other genes displayed EAE-specific regulation. *Dnttip* exon 1 was not determined due to technical issues. * p<0.05 using a Mann-Whitney non-parametric test. Error bars represent standard deviation.

doi:10.1371/journal.pone.0007773.g003

Table 2. Alternatively spliced genes between DA and PVG cells after MOG re-stimulation.

Ensembl ID	Transcript ID	Gene Symbol	p-value	Differential Exon	Reduced Strain	Interpro Domain	Domain Function
T00000032767	7271202	Itpr2	6.41E-42	15	PVG	-	No specific domain
T00000014289	7283429	Nsmaf	1.29E-18	12	DA	IPR000409	Beige/Beach, unknown
T00000005811	7107800	Usf1	7.80E-13	7	PVG	IPR001092	Basic Helix-Loop-Helix, DNA binding + transcription
T00000040922	7173094	Rock1	6.34E-12	12	PVG	IPR011009	Protein kinase-like, phosphotransfer
T00000026725	7282342	Cpsf3l	5.18E-11	5	PVG	IPR001279	Beta-lactamase-like, hydrolase
T00000016224	7055841	Tmem41b	1.96E-09	6	DA	-	Transmembrane Helix
T00000059034	7185469	Ddx19a	2.79E-08	10	DA	-	No specific domain
T00000019338	7056128	Btbd10	3.32E-07	5	PVG	IPR003131	Potassium channel, voltage dependent
T00000001868	7102483	Slc24a6	4.44E-05	8	DA	-	No specific domain

Differential Exon - alternatively spliced between strains; Reduced Strain - lower expression of indicated exon; Interpro Domain - protein domain encoded in alternatively spliced exon.
doi:10.1371/journal.pone.0007773.t002

expressed genes (Table S5). DAVID clustering analyses revealed that similar GO pathways were regulated in both strains. Both DA and PVG respond to stimulus by regulating metabolism, transport, kinase activity, transcription and apoptosis, which ultimately control the immune response (Tables S6 and S7). Although similar pathways were regulated in both strains, some of the genes associated with these clusters were strain specific. For example, sterol metabolism was highly enriched when comparing day 7 *ex vivo* versus MOG re-stimulated conditions for each strain separately, with 16 common associated genes. However, *Mvd*, *Oprs1* and *Hmgcs1* were identified only for DA, while *Osbpl5* and *Ebp* were differentially expressed only for PVG.

Candidate Genes for EAE QTLs

Several of the differentially expressed genes and an alternatively spliced gene identified in this study overlap with known QTLs between DA and PVG (Table 6). We confirmed the Affymetrix data using qPCR for 4 of these targets: *Il4ra*, *Klrc3*, *App* and *Mfsd4* (Figure 4). These genes can be considered as candidate genes governing EAE susceptibility in these regions.

Discussion

We investigated the induction phase and autoreactive cell effector functions during EAE between susceptible DA and

resistant PVG inbred rat strains using whole genome expression profiling of peripheral lymphatic tissue. Our aim was to assess the role of alternative splicing and to identify genes that were responsible for susceptibility to the disease. We hypothesized that alternative splicing, a mechanism that widely occurs between tissues and across time [29], is an important mechanism involved in disease regulation. Additionally, we sought to identify candidate genes and pathways responsible for genetically-determined EAE susceptibility, some of which may also regulate the human disease, MS.

Our study identified a total of 13 alternative spliced genes between susceptible and resistant strains. This result is likely an underestimation of the true event number with many false-negatives (Type II error) due to at least two reasons. Firstly, we have used a mixed population of lymph node cells, which could mask the contribution of individual cell type specific alternative splicing. Secondly, we employed several methods to increase stringency, as most of the alternative splicing detection methods suffer from high false positive detection rates [30]. We observed genes that were differentially spliced between EAE-susceptible and -resistant rat strains during disease induction and effector phases. When examining the missing exons we determined that the isoforms for many genes are missing integral protein domains, thus providing support that these differences functionally contribute to disease susceptibility. The spliced genes are involved in several

Table 3. DAVID enriched GO terms of differentially expressed genes between DA and PVG for day 7 *ex vivo* lymph nodes.

Category	Representative GO Term	Genes	Count/List	Pop Hits/Total	Fold Enrichment	p-value
GO:BP	GO:0030154~cell differentiation	Nuak2, Agrn, Cd5, Nrp2, App, Il2ra, Actn1, Cstb, F2r, Rps6ka2, Igf1r, Capn5, Apbb1, Anxa1, Zfp37,	18/83	1584/12762	1.75	2.21E-02
GO:BP	GO:0006493~protein amino acid O-linked glycosylation	Pomgnt1, Galnt11, Galnt10,	3/83	17/12762	27.13	5.21E-03
GO:BP	GO:0042981~regulation of apoptosis	Nuak2, Cd5, App, Igf1r, Il2ra, Actn1, Anxa1, F2r, Cstb,	9/83	525/12762	2.64	1.93E-02
GO:BP	GO:0007268~synaptic transmission	Gnai1, Vdac3, Agrn, Sv2b, App, Nsg1, Stx3,	8/83	446/12762	2.76	3.93E-02
GO:BP	GO:0043062~extracellular structure organization and biogenesis	Agrn, App, Apbb1, F2r,	4/83	98/12762	6.28	2.51E-02

GO:BP - Gene Ontology, Biological Process; p value - modified Fischer Exact Test.
doi:10.1371/journal.pone.0007773.t003

Table 4. GSEA enriched gene sets between DA and PVG.

NAME	Top 10 genes	Source	SIZE	NOM p-val	FDR q-val
DA vs. PVG day 7 ex vivo significant pathways					
SULFOTRANSFERASE_ACTIVITY	Chst9, Chst7, Chst10, Chst13, Tpst1, Hs3st5, Chst3, Chst5, Chst8, Chst4	GO	20	0	0.03662996
HSA04080_NEUROACTIVE_LIGAND_RECEPTOR_INTERACTION	Ptger3, P2ry14, Gzma, Uts2R, Prl, Mtnr1a, Ghnr, P2ry4, Grin2B, Htr1B	KEGG	205	0	0.0560383
SUBSTRATE_SPECIFIC_CHANNEL_ACTIVITY	Kcna1, Cacng5, Kcnj15, Kcna4, Nmur2, Kcnb2, Kcne2, P2rx3, Kcnk4, Scn2b	GO	131	0	0.07680687
DA vs. PVG MOG restimulation significant pathways					
VOLTAGE_GATED_POTASSIUM_CHANNEL_ACTIVITY	Kcnj4, Kcnj3, Kcnj1, Kcnip2, Kcna5, Kcnh1, Kcnj10, Kcna2, Kcnc1, Kcnj15	GO	31	0	0.014385469
FEEDING_BEHAVIOR	Mc4r, Npy, Ghrl, Htr2c, Lep, Npw, Mchr1, Calr2, Hcrtr2, Ppyr1	GO	21	0	0.015389259
POTASSIUM_ION_TRANSPORT	Kcnj4, Kcnj3, Kcnj3, Kcnj1, Kcnj11, Kcnip2, Kcna5, Kcnh1, Kcnj10, Kcnf1	GO	49	0	0.027649486
POTASSIUM_CHANNEL_ACTIVITY	Kcnj4, Kcnj3, Kcnj1, Kcnip2, Kcna5, Kcnh1, Kcnj10, Kcna2, Kcnc1, Kcnj15	GO	41	0	0.02914241
HORMONE_ACTIVITY	Gh1, Npy, Ghrl, Igf1, Stc1, Cga, Nppb, Calcb, Chgb, Pnoc	GO	36	0	0.029265244
GPCRDB_CLASS_A_RHODOPSIN_LIKE	Nmur1, Gpr85, Chrm5, Gpr83, Drd2, Mc4r, Fpr1, Gpr37, P2ry1, Grpr	GenMAPP	133	0	0.032977927
RESPONSE_TO_NUTRIENT_LEVELS	Nuak2, Npy, Ghrl, Lep, Stc1, Sst, Cdkn2b, Alb	GO	26	0.001677852	0.034934502
INTERMEDIATE_FILAMENT_CYTOSKELETON	Gfap, Drd2, Nefl, Krt31, Pkp1, Upp2, Krt2	GO	18	0.001658375	0.036004912
VOLTAGE_GATED_POTASSIUM_CHANNEL_COMPLEX	Kcnj4, Kcnj3, Kcnj1, Kcna5, Kcnh1, Kcna2, Kcnc1, Kcnj8, Kcns1, Kcnn3	GO	35	0	0.03604953
RESPONSE_TO_EXTRACELLULAR_STIMULUS	Nuak2, Npy, Ghrl, Lep, Stc1, Sst, Cdkn2b, Alb	GO	28	0.001712329	0.03640272
STRUCTURAL_CONSTITUENT_OF_CYTOSKELETON	Actl7a, Gfap, Nefl, Krt31, Sorbs3, Ppl, Des, Actl7b, Mapt, Krt2	GO	42	0	0.036414582
INTERMEDIATE_FILAMENT	Gfap, Drd2, Nefl, Krt31, Pkp1, Upp2, Krt2	GO	18	0.00172117	0.036638036
HSA04080_NEUROACTIVE_LIGAND_RECEPTOR_INTERACTION	Nmur1, Prss1, Npffr2, Chrm5, Gpr83, Gh1, Taar2, Drd2, Mc4R, Fpr1	KEGG	205	0	0.037446167
SYSTEM_PROCESS	Nmur1, Omp, Six3, Gja3, Sspn, Pmp22, Drd2, Npy, Nrl, Kcnj1	GO	441	0	0.038417198
HSA01430_CELL_COMMUNICATION	Chad, Gja3, Krt35, Krt34, Ibsp, Krt25, Krt31, Nes, Krt86, Krt40	KEGG	96	0	0.038440228
SYNAPTIC_TRANSMISSION	Omp, Pmp22, Drd2, Npy, Ghrl, Kcnip1, Htr2c, Pcdhb13, Pcdhb6, Htr1b	GO	151	0	0.038810864
NEUROLOGICAL_SYSTEM_PROCESS	Nmur1, Omp, Six3, Gja3, Pmp22, Drd2, Npy, Nrl, Ghrl, Kcnip1	GO	290	0	0.039604984
CARBOHYDRATE_TRANSPORT	Gh1, Pbbp, Ednra, Slc2a5	GO	15	0.001675042	0.046175405

Top 10 genes – top 10 ranking genes belonging to a gene set; source – source for the gene set; size – number of genes in a gene set; NOM p-val – nominal p value; FDR q-val – false discovery rate.

doi:10.1371/journal.pone.0007773.t004

general signaling and transcriptional regulatory mechanisms that were identified in this study. *Rasa1* and *Rock1* alternative splicing was EAE-specific and could control cell motility, proliferation and differentiation through Ras and Rho GTPases respectively [31,32]. Additionally, *Nab1*, *Cpsf3l*, *Btd10* and *Uyf1* all modulate transcription [33,34,35,36]. However, further investigation is required to determine the precise effect these different isoforms have during EAE induction. Interestingly, 5 of the 10 genes identified (this excludes *Ddx19a*, which could not be reproduced likely due to a SNP affecting hybridization) as alternatively spliced in day 7 lymph nodes were also spliced after MOG re-stimulation. This result indicates that these isoforms are constitutive during disease and may govern disease-driving mechanisms.

Expressional regulation is an important mechanism modulating biological processes. Many genes are differentially expressed

during disease, providing markers of disease progression and indications of pathways and mechanisms that are deregulated. We identified 206 genes that were differentially expressed between the two stains in day 7 post-immunization lymph nodes. Of those genes, *Cd5*, *Il18r1* and *Il2ra* are known encephalomyelitis candidates [7,37,38]. All three are strongly up-regulated in DA lymph nodes. Disease-driving regulated genes in EAE are often related to the immune system and govern processes including antigen processing, transcription, cytokines and cellular attraction, adhesion, division and death. Our study supports this body of evidence but also extends the findings to propose new candidates governing autoimmunity that are implicated in glycosylation (*Pomgt1*, *Galnt11* and *Galnt10*). Our study focused on the periphery where protein glycosylation may affect receptor signaling and thereby alter disease susceptibility [39]. Additionally, pathogenic

Table 5. DAVID enriched GO terms of differentially expressed genes between DA and PVG for MOG re-stimulated cells.

Category	Representative GO Term	First 10 Genes	Count/ List	Pop Hits/ Total	Fold Enrichment	p-value
GO:BP	GO:0051234~establishment of localization	Drd2, Arfgap1, Camk2d, Atp10a, Cxcr4, P2rx4, Trpm6, Tpo1, Slc27a1, Dirc2	25/76	2420/12762	1.73	4.77E-03
GO:BP	GO:0012501~programmed cell death	Cd2, Litaf, Nuak2, Cd5, App, Fgf2, Igf1r, Il2ra, Cxcr4, F2r	11/76	690/12762	2.68	6.88E-03
GO:BP	GO:0006464~protein modification process	Pigq, Nuak2, Pomgnt1, Art2b, Camk2d, St8sia1, Cry2, Uhrf1, Insr, Atg7	19/76	1403/12762	2.27	1.03E-03
GO:BP	GO:0030154~cell differentiation	Litaf, Nuak2, Cd5, Nrp2, App, Il2ra, Sort1, Cxcr4, F2r, Cd2	16/76	1584/12762	1.70	4.05E-02
GO:BP	GO:0046649~lymphocyte activation	Cd2, Cd5, Nbn, Il2ra, Cxcr4	4/76	105/12762	6.40	2.38E-02
GO:BP	GO:0008152~metabolic process	Drd2, Gfpt2, Cdo1, St8sia1, Cybrd1, Lmo7, Chst10, Trpm6, Capn5, Khdrbs3	51/76	7051/12642	1.21	2.91E-02
GO:BP	GO:0000902~cell morphogenesis	Nrp2, App, Fgf2, Igf1r, Camk2d, Socs2, Atp10a, Cxcr4	8/76	468/127642	2.87	1.98E-02
GO:BP	GO:0042110~T cell activation	Cd2, Cd5, Il2ra, Cxcr4	4/76	105/12762	6.40	2.38E-02
GO:BP	GO:0048856~anatomical structure development	Drd2, Nrp2, App, Camk2d, Il2ra, Csrp1, Sort1, Atp10a, Hsd11b1, Insr	19/76	1988/12762	1.60	3.69E-02

GO:BP - Gene Ontology, Biological Process; p value - modified Fischer Exact Test.
doi:10.1371/journal.pone.0007773.t005

glycosylated antigens are generated during EAE and antibodies against these targets perturb disease [40].

After MOG re-stimulation we identified 144 genes that were differentially expressed between the two strains. One the genes strongly up-regulated in DA lymph nodes was *Havcr1/Tim1*, which was also increased in cerebrospinal fluid mononuclear cells of patients with MS [41]. GSEA analysis identified up-regulation of several members of the inward rectifier potassium channel family, including *Kcnj1* and *Kcnj4*, in PVG cells, suggesting that these channels may play a protective role in EAE. *Kcnj4* (or *Kir2.3*) has recently been linked with protection against neurodegeneration in a cell model of Parkinson's disease [42], although its role in the immune system is currently unknown. There is strong interest in targeting potassium channels for MS therapy and several clinical trials related to the therapeutic targeting of voltage-gated K⁺ (K_v) channels in MS are ongoing [43]. These therapies will likely not

only target nervous tissue and conductance, but also lymphocyte proliferation [44,45]. Additionally, K_v channels regulate immune synapses in the periphery where antigen presentation occurs and lymphocyte function is determined [46].

It should be noted that stringent criteria were used for all our analysis. We chose this approach to simplify interpretation of the data, reduce the occurrence of false positives and provide strong novel EAE susceptibility candidates. Because of the stringent criteria, we find that only a portion of the genes from our previous study [7], which utilized qPCR methods, pass the 5% FDR cut-off, including *Il18r1*, *Il2ra* and *FoxP3*. However, genes that do not pass a FDR of 5% in this study, including *Il17f*, *Il7r*, *Stat4* and *Tnf*, are consistently differentially expressed at a lower threshold (p<0.05). When examining known MS candidates we found that both *Il7r* and *Il2ra* were confirmed as being differentially expressed between DA and PVG in day 7 *ex vivo* lymph nodes (p=0.04 and

Table 6. Candidate genes for EAE quantitative trait loci.

QTL	Chromosome	Position (Mb)	Candidate Genes	Related Publication
"Eae31"	1	183.9–193.1	Il4ra, Acadsb	
Unnamed	1	234.5–268	Lipa, Ifit1, Pdlim1, RGD1303232	
'Eae24-27"	4	44–116.6	<u>Scrn1</u> , LOC681217, Gimap4, Reg3g, Tspan33, Chn2	Becanovic et al., 2003
Eae20	4	157–160.5	<u>Slc6a12</u>	Jagodic et al., 2005
Eae22	4	~167	<u>Klrc3</u>	Jagodic et al., 2005
Unnamed	5	125.6–173	Dmrtb1, Spata6, Pomgnt1, Csf3r, Agrn, Acot7, Cpsf3l	
'Eae16"	8	81.4–102.9	<u>Lrrc</u> , <u>Plscr2</u>	
Eae18a	10	55.8–62.7	Plscr3, Zmynd15, Eno3, <u>Cldn7</u> , <u>Kif1c</u>	Jagodic et al., 2004
Unnamed	11	20–70	<u>App</u> , Mx1, Retnlg, Cd200r1, Parp9, Dirc2	
'Eae17"	13	39.6–55.4	<u>Mfsd4</u> , Nuak2, Pik3c2b, Chi2l1, Cfh, Cxcr4	
Unnamed	14	0–26.4	Naaa, <u>Slc4a4</u>	
Eae19	15	83.3–97.7	Lmo7, <u>Spry2</u>	Sheng et al., 2005
'Eae23"	17	36–66	Pols	

QTLs in quotations or unnamed are based on personal communication; Genes - differentially expressed between DA and PVG in day 7 *ex vivo* lymph node cells; Genes - differentially expressed in MOG re-stimulated cells; Genes - differentially expressed in both *ex vivo* and re-stimulated conditions; **Genes** - alternatively spliced.
doi:10.1371/journal.pone.0007773.t006

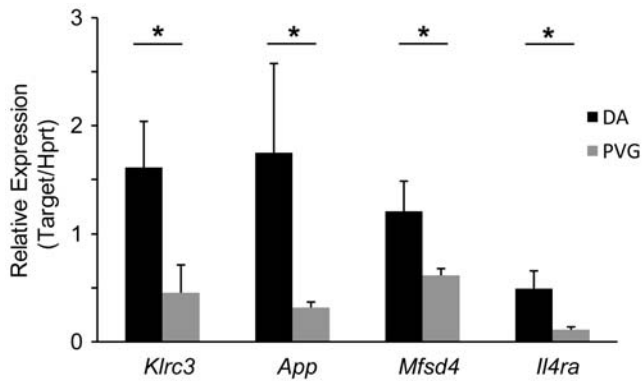


Figure 4. Quantitative PCR confirmation of candidate genes for EAE QTLs. Relative expression compared to *Hprt* of *Klrc3*, *App*, *Mfsd4* and *Il4ra* from DA (n=4) and PVG (n=4) female rat lymph nodes, 7 days post-immunization. DA lymph nodes had higher expression of all 4 targets, confirming the Affymetrix data. * $p < 0.05$ using a Mann-Whitney non-parametric test. Error bars represent standard deviation. doi:10.1371/journal.pone.0007773.g004

$p = 8 \times 10^{-5}$, respectively). We also determined differential expression of *Evi5* ($p = 0.03$) in *ex vivo* cells and *Irf8/Icsbp1* ($p = 0.02$) following MOG re-stimulation [47,48]. These results provide further evidence that MOG-induced EAE in DA rats is a relevant model for study of MS. However, not all MS candidate molecules are transcriptionally regulated at this time-point in this tissue. Candidate genes including *KIF1β* [49], *RPL5* [50], *IRF5* [47], *CD226* [51], *CD6* and *TNFRSF1A* [48] were equally expressed between susceptible and resistant strains.

Several studies have employed linkage analysis with QTL mapping to identify genomic regions regulating EAE in rats [52,53,54,55,56]. However, identification of the genetic polymorphisms responsible for disease susceptibility has been a slow process. We combined QTL mapping and expression profiling, a strategy that has been successful at identifying the molecular basis of a number of QTLs in rats [57,58,59,60]. We have identified numerous differentially expressed and alternatively spliced genes overlapping previously described QTLs for EAE between DA and PVG and confirmed several of them using qPCR. One candidate from our study, *Cxcr4*, is involved in leukocyte trafficking and has previously been implicated in EAE [61]. Another candidate, *Klrc3*, encodes an activating natural killer (NK) cell receptor, which could potentially regulate NK cell involvement in EAE [62,63]. We propose these and other genes as candidates in the respective genetic regions and believe that directed study will help identify pathways regulated during autoimmune reactions, giving further insight into human MS.

Supporting Information

Figure S1 Eleven genes alternatively spliced between DA and PVG day 7 *ex vivo* lymph node cells, as presented from Partek's gene viewer (A-K). The average RMA normalized intensity values and standard error for each probe-set, are shown for EAE-susceptible DA (blue) and EAE-resistant PVG (red) rat strains. The Log₂ intensity scale is shown on the right axis. Arrows designate alternatively spliced exons. Found at: doi:10.1371/journal.pone.0007773.s001 (1.72 MB DOC)

Figure S2 Nine genes alternatively spliced between DA and PVG MOG re-stimulated lymph node cells, as presented from Partek's gene viewer (A-I). The average RMA normalized

intensity values and standard error for each probe-set are shown for EAE-susceptible DA (blue) and EAE-resistant PVG (red) rat strains. The Log₂ intensity scale is shown on the right-hand axis. Arrows designate alternatively spliced exons.

Found at: doi:10.1371/journal.pone.0007773.s002 (1.05 MB DOC)

Figure S3 Alternative splicing genes from *ex vivo* vs. re-stimulated conditions, as represented from Partek's gene viewer. DA shows down-regulation of the 3' end of *Chrne* after MOG re-stimulation (A). PVG shows down-regulation of the 5' end of *Crem* after re-stimulation (B). The average RMA normalized intensity values and standard error for each probe-set are shown. Arrows designate alternatively spliced exons.

Found at: doi:10.1371/journal.pone.0007773.s003 (0.54 MB DOC)

Figure S4 *Ddx19a* is an example of an alternatively spliced false-positive induced by a SNP. (A) Sequencing exon 10 of *Ddx19a* identified a SNP (arrows) in probe-set 5733439 between DA and PVG. (B) Relative expression compared to *Hprt* for *Ddx19a* determined no difference between DA (n=4) and PVG (n=4) for exon 10, the putative alternatively spliced exon. Error bars represent standard deviation.

Found at: doi:10.1371/journal.pone.0007773.s004 (0.28 MB PDF)

Table S1 Primer sequences for SYBR quantitative real-time PCR targets.

Found at: doi:10.1371/journal.pone.0007773.s005 (0.02 MB DOC)

Table S2 Differentially regulated transcripts between DA and PVG in day 7 *ex vivo* lymph nodes. 138 transcripts were upregulated and 68 downregulated using DA as reference at a 5% FDR cut-off margin.

Found at: doi:10.1371/journal.pone.0007773.s006 (0.04 MB DOC)

Table S3 Differentially regulated transcripts between DA and PVG in MOG re-stimulated cells. 90 transcripts were upregulated and 54 downregulated using DA as reference at a 5% FDR cut-off margin.

Found at: doi:10.1371/journal.pone.0007773.s007 (0.04 MB DOC)

Table S4 Differentially regulated transcripts comparing DA day 7 *ex vivo* and MOG re-stimulated conditions. 470 transcripts were upregulated and 433 downregulated using day 7 *ex vivo* as reference at a 5% FDR cut-off margin.

Found at: doi:10.1371/journal.pone.0007773.s008 (0.13 MB DOC)

Table S5 Differentially regulated transcripts comparing PVG day 7 *ex vivo* and MOG re-stimulated conditions. 637 transcripts were upregulated and 719 downregulated using day 7 *ex vivo* as reference at a 5% FDR cut-off margin.

Found at: doi:10.1371/journal.pone.0007773.s009 (0.18 MB DOC)

Table S6 DAVID functional clustering results of DA day 7 *ex vivo* and DA MOG re-stimulated conditions.

Found at: doi:10.1371/journal.pone.0007773.s010 (0.02 MB DOC)

Table S7 DAVID functional clustering results of PVG day 7 *ex vivo* and PVG MOG re-stimulated conditions.

Found at: doi:10.1371/journal.pone.0007773.s011 (0.03 MB DOC)

Author Contributions

Conceived and designed the experiments: AG KM RAH MJ TJA TO. Performed the experiments: AG KM CF. Analyzed the data: AG KM CF.

Contributed reagents/materials/analysis tools: TJA TO. Wrote the paper: AG KM.

References

- Compston A, Coles A (2008) Multiple sclerosis. *Lancet* 372: 1502–1517.
- Millefiorini E, Gasperini C, Pozzilli C, D'Andrea F, Bastianello S, et al. (1997) Randomized placebo-controlled trial of mitoxantrone in relapsing-remitting multiple sclerosis: 24-month clinical and MRI outcome. *J Neurol* 244: 153–159.
- Cross AH, Stark JL, Lauber J, Ramsbottom MJ, Lyons JA (2006) Rituximab reduces B cells and T cells in cerebrospinal fluid of multiple sclerosis patients. *J Neuroimmunol* 180: 63–70.
- Müller DH, Khan OA, Sheremata WA, Blumhardt LD, Rice GP, et al. (2003) A controlled trial of natalizumab for relapsing multiple sclerosis. *N Engl J Med* 348: 15–23.
- Dutta R, Trapp BD (2007) Pathogenesis of axonal and neuronal damage in multiple sclerosis. *Neurology* 68: S22–31; discussion S43–54.
- Storch MK, Steffler A, Brehm U, Weissert R, Wallstrom E, et al. (1998) Autoimmunity to myelin oligodendrocyte glycoprotein in rats mimics the spectrum of multiple sclerosis pathology. *Brain Pathol* 8: 681–694.
- Thessen Hedreul M, Gillett A, Olsson T, Jagodic M, Harris RA (2009) Characterization of Multiple Sclerosis candidate gene expression kinetics in rat experimental autoimmune encephalomyelitis. *J Neuroimmunol*.
- O'Connor RA, Prendergast CT, Sabatos CA, Lau CW, Leech MD, et al. (2008) Cutting edge: Th1 cells facilitate the entry of Th17 cells to the central nervous system during experimental autoimmune encephalomyelitis. *J Immunol* 181: 3750–3754.
- Stromnes IM, Cerretti LM, Liggitt D, Harris RA, Goverman JM (2008) Differential regulation of central nervous system autoimmunity by T(H)1 and T(H)17 cells. *Nat Med* 14: 337–342.
- Mueller AM, Pedre X, Stempf I, Kleiter I, Couillard-Despres S, et al. (2008) Novel role for SLPI in MOG-induced EAE revealed by spinal cord expression analysis. *J Neuroinflammation* 5: 20.
- Carmody RJ, Hilliard B, Maguschak K, Chodosh LA, Chen YH (2002) Genomic scale profiling of autoimmune inflammation in the central nervous system: the nervous response to inflammation. *J Neuroimmunol* 133: 95–107.
- Ibrahim SM, Mix E, Botcher T, Koczan D, Gold R, et al. (2001) Gene expression profiling of the nervous system in murine experimental autoimmune encephalomyelitis. *Brain* 124: 1927–1938.
- Achiron A, Feldman A, Mandel M, Gurevich M (2007) Impaired expression of peripheral blood apoptotic-related gene transcripts in acute multiple sclerosis relapse. *Ann N Y Acad Sci* 1107: 155–167.
- Arthur AT, Armati PJ, Bye C, Heard RN, Stewart GJ, et al. (2008) Genes implicated in multiple sclerosis pathogenesis from consilience of genotyping and expression profiles in relapse and remission. *BMC Med Genet* 9: 17.
- Avasarala JR, Chittur SV, George AD, Tine JA (2008) Microarray analysis in B cells among siblings with/without MS - role for transcription factor TCF2. *BMC Med Genomics* 1: 2.
- Lundmark F, Duvefelt K, Iacobaeus E, Koekum I, Wallstrom E, et al. (2007) Variation in interleukin 7 receptor alpha chain (IL7R) influences risk of multiple sclerosis. *Nat Genet* 39: 1108–1113.
- Gregory SG, Schmidt S, Seth P, Oksenberg JR, Hart J, et al. (2007) Interleukin 7 receptor alpha chain (IL7R) shows allelic and functional association with multiple sclerosis. *Nat Genet* 39: 1083–1091.
- Amor S, Groome N, Linington C, Morris MM, Dornmair K, et al. (1994) Identification of epitopes of myelin oligodendrocyte glycoprotein for the induction of experimental allergic encephalomyelitis in SJL and Biozzi AB/H mice. *J Immunol* 153: 4349–4356.
- Parkinson H, Kapushesky M, Shojatalab M, Abeygunawardena N, Coulson R, et al. (2007) ArrayExpress—a public database of microarray experiments and gene expression profiles. *Nucleic Acids Res* 35: D747–750.
- Irizarry RA, Hobbs B, Collin F, Beazer-Barclay YD, Antonellis KJ, et al. (2003) Exploration, normalization, and summaries of high density oligonucleotide array probe level data. *Biostatistics* 4: 249–264.
- Della Beffa C, Cordero F, Calogero RA (2008) Dissecting an alternative splicing analysis workflow for GeneChip Exon 1.0 ST Affymetrix arrays. *BMC Genomics* 9: 571.
- Genleman RC, Carey VJ, Bates DM, Bolstad B, Dettling M, et al. (2004) Bioconductor: open software development for computational biology and bioinformatics. *Genome Biol* 5: R80.
- Sanges R, Cordero F, Calogero RA (2007) oneChannelGUI: a graphical interface to Bioconductor tools, designed for life scientists who are not familiar with R language. *Bioinformatics* 23: 3406–3408.
- Benjamini YaH, Y (1995) Controlling the false discovery rate—a practical and powerful approach to multiple testing. *JR Statist Soc* 57: 289–300.
- Dennis G Jr, Sherman BT, Hosack DA, Yang J, Gao W, et al. (2003) DAVID: Database for Annotation, Visualization, and Integrated Discovery. *Genome Biol* 4: P3.
- Huang da W, Sherman BT, Lempicki RA (2009) Systematic and integrative analysis of large gene lists using DAVID bioinformatics resources. *Nat Protoc* 4: 44–57.
- Subramanian A, Tamayo P, Mootha VK, Mukherjee S, Ebert BL, et al. (2005) Gene set enrichment analysis: a knowledge-based approach for interpreting genome-wide expression profiles. *Proc Natl Acad Sci U S A* 102: 15545–15550.
- Benovoy D, Kwan T, Majewski J (2008) Effect of polymorphisms within probe-target sequences on oligonucleotide microarray experiments. *Nucleic Acids Res* 36: 4417–4423.
- Wang ET, Sandberg R, Luo S, Khrebtkova I, Zhang L, et al. (2008) Alternative isoform regulation in human tissue transcriptomes. *Nature* 456: 470–476.
- Bemmo A, Benovoy D, Kwan T, Gaffney DJ, Jensen RV, et al. (2008) Gene expression and isoform variation analysis using Affymetrix Exon Arrays. *BMC Genomics* 9: 529.
- Mor A, Philips MR (2006) Compartmentalized Ras/MAPK signaling. *Annu Rev Immunol* 24: 771–800.
- Nagamatsu Y, Rikitake Y, Takahashi M, Deki Y, Ikeda W, et al. (2008) Roles of Nect-5/poliiovirus receptor and Rho-associated kinase (ROCK) in the regulation of transformation of integrin alpha(V)beta(3)-based focal complexes into focal adhesions. *J Biol Chem* 283: 14532–14541.
- Russo MW, Severson BR, Milbrandt J (1995) Identification of NAB1, a repressor of NGFI-A- and Krox20-mediated transcription. *Proc Natl Acad Sci U S A* 92: 6873–6877.
- Baillat D, Hakimi MA, Naar AM, Shilatfard A, Cooch N, et al. (2005) Integrator, a multiprotein mediator of small nuclear RNA processing, associates with the C-terminal repeat of RNA polymerase II. *Cell* 123: 265–276.
- Chen J, Xu J, Ying K, Cao G, Hu G, et al. (2004) Molecular cloning and characterization of a novel human BTB domain-containing gene, BTBD10, which is down-regulated in glioma. *Gene* 340: 61–69.
- Sawadogo M, Roeder RG (1985) Interaction of a gene-specific transcription factor with the adenovirus major late promoter upstream of the TATA box region. *Cell* 43: 165–175.
- Gutcher I, Ulrich E, Wolter K, Prinz M, Becher B (2006) Interleukin 18-independent engagement of interleukin 18 receptor-alpha is required for autoimmune inflammation. *Nat Immunol* 7: 946–953.
- Sun D, Branum K, Sun Q (1992) Prevention of experimental autoimmune encephalomyelitis in Lewis rats by treatment with an anti-rat CD5 antibody (OX19). *Cell Immunol* 145: 263–271.
- Walter S, Fassbender K, Gulbins E, Liu Y, Rieschel M, et al. (2002) Glycosylation processing inhibition by castanospermine prevents experimental autoimmune encephalomyelitis by interference with IL-2 receptor signal transduction. *J Neuroimmunol* 132: 1–10.
- Marta CB, Oliver AR, Sweet RA, Pfeiffer SE, Ruddle NH (2005) Pathogenic myelin oligodendrocyte glycoprotein antibodies recognize glycosylated epitopes and perturb oligodendrocyte physiology. *Proc Natl Acad Sci U S A* 102: 13992–13997.
- Khademi M, Illes Z, Gielen AW, Marta M, Takazawa N, et al. (2004) T Cell Ig- and mucin-domain-containing molecule-3 (TIM-3) and TIM-1 molecules are differentially expressed on human Th1 and Th2 cells and in cerebrospinal fluid-derived mononuclear cells in multiple sclerosis. *J Immunol* 172: 7169–7176.
- Wang G, Zeng J, Shen CY, Wang ZQ, Chen SD (2008) Overexpression of Kir2.3 in PC12 cells resists rotenone-induced neurotoxicity associated with PKC signaling pathway. *Biochem Biophys Res Commun* 374: 204–209.
- Judge SI, Bever CT Jr (2006) Potassium channel blockers in multiple sclerosis: neuronal Kv channels and effects of symptomatic treatment. *Pharmacol Ther* 111: 224–259.
- DeCoursey TE, Chandy KG, Gupta S, Cahalan MD (1984) Voltage-gated K⁺ channels in human T lymphocytes: a role in mitogenesis? *Nature* 307: 465–468.
- Lee SC, Sabath DE, Deutsch C, Prystowsky MB (1986) Increased voltage-gated potassium conductance during interleukin 2-stimulated proliferation of a mouse helper T lymphocyte clone. *J Cell Biol* 102: 1200–1208.
- Panyi G, Vamosi G, Bacso Z, Bagdany M, Bodnar A, et al. (2004) Kv1.3 potassium channels are localized in the immunological synapse formed between cytotoxic and target cells. *Proc Natl Acad Sci U S A* 101: 1285–1290.
- Hoppenbrouwers IA, Aulchenko YS, Ebers GC, Ramagopalan SV, Oostra BA, et al. (2008) EV15 is a risk gene for multiple sclerosis. *Genes Immun* 9: 334–337.
- De Jager PL, Jia X, Wang J, de Bakker PI, Ottoboni L, et al. (2009) Meta-analysis of genome scans and replication identify CD6, IRF8 and TNFRSF1A as new multiple sclerosis susceptibility loci. *Nat Genet* 41: 776–782.
- Aulchenko YS, Hoppenbrouwers IA, Ramagopalan SV, Broer L, Jafari N, et al. (2008) Genetic variation in the KIF1B locus influences susceptibility to multiple sclerosis. *Nat Genet* 40: 1402–1403.
- Rubio JP, Stankovich J, Field J, Tubridy N, Marriott M, et al. (2008) Replication of KIAA0350, IL2RA, RPL5 and CD58 as multiple sclerosis susceptibility genes in Australians. *Genes Immun* 9: 624–630.
- Hafler JP, Maier LM, Cooper JD, Plagnol V, Hinks A, et al. (2009) CD226 Gly307Ser association with multiple autoimmune diseases. *Genes Immun* 10: 5–10.

52. Becanovic K, Backdahl L, Wallstrom E, Aboul-Enein F, Lassmann H, et al. (2003) Paradoxical effects of arthritis-regulating chromosome 4 regions on myelin oligodendrocyte glycoprotein-induced encephalomyelitis in congenic rats. *Eur J Immunol* 33: 1907–1916.
53. Jagodic M, Becanovic K, Sheng JR, Wu X, Backdahl L, et al. (2004) An advanced intercross line resolves Eae18 into two narrow quantitative trait loci syntenic to multiple sclerosis candidate loci. *J Immunol* 173: 1366–1373.
54. Sheng JR, Jagodic M, Dahlman I, Becanovic K, Nohra R, et al. (2005) Eae19, a new locus on rat chromosome 15 regulating experimental autoimmune encephalomyelitis. *Genetics* 170: 283–289.
55. Jagodic M, Marta M, Becanovic K, Sheng JR, Nohra R, et al. (2005) Resolution of a 16.8-Mb autoimmunity-regulating rat chromosome 4 region into multiple encephalomyelitis quantitative trait loci and evidence for epistasis. *J Immunol* 174: 918–924.
56. Jagodic M, Olsson T (2006) Combined-cross analysis of genome-wide linkage scans for experimental autoimmune encephalomyelitis in rat. *Genomics* 88: 737–744.
57. Petretto E, Sarwar R, Grieve I, Lu H, Kumaran MK, et al. (2008) Integrated genomic approaches implicate osteoglycin (Ogn) in the regulation of left ventricular mass. *Nat Genet* 40: 546–552.
58. Monti J, Fischer J, Paskas S, Heinig M, Schulz H, et al. (2008) Soluble epoxide hydrolase is a susceptibility factor for heart failure in a rat model of human disease. *Nat Genet* 40: 529–537.
59. Emilsson V, Thorleifsson G, Zhang B, Leonardson AS, Zink F, et al. (2008) Genetics of gene expression and its effect on disease. *Nature* 452: 423–428.
60. Behmoaras J, Bhargal G, Smith J, McDonald K, Mutch B, et al. (2008) Jund is a determinant of macrophage activation and is associated with glomerulonephritis susceptibility. *Nat Genet* 40: 553–559.
61. Jiang Y, Salafra MN, Adhikari S, Xia Y, Feng L, et al. (1998) Chemokine receptor expression in cultured glia and rat experimental allergic encephalomyelitis. *J Neuroimmunol* 86: 1–12.
62. Zhang BN, Yamamura T, Kondo T, Fujiwara M, Tabira T (1997) Regulation of experimental autoimmune encephalomyelitis by natural killer (NK) cells. *Journal of Experimental Medicine* 186: 1677–1687.
63. Matsumoto Y, Kohyama K, Aikawa Y, Shin T, Kawazoe Y, et al. (1998) Role of natural killer cells and TCR-gamma-delta T cells in acute autoimmune encephalomyelitis. *European Journal of Immunology* 28: 1681–1688.